

# Joint Phase Time Array: Opportunities, Challenges, and System Design Considerations

Young-Han Nam, *Member, IEEE*, Ahmad AlAmmouri, *Member, IEEE*, Jianhua Mo, *Senior Member, IEEE* and Jianzhong Charlie Zhang, *Fellow, IEEE*

**Abstract**— This paper presents a novel approach to designing millimeter-wave (mmWave) cellular communication systems, based on joint phase time array (JPTA) radio frequency (RF) frontend architecture. JPTA architecture comprises time-delay components appended to conventional phase shifters, which offer extra degrees of freedom to be exploited for designing frequency-selective analog beams. Hence, a mmWave device equipped with JPTA can receive and transmit signals in multiple directions in a single time slot per RF chain, one direction per frequency subband, which alleviates the traditional constraint of one analog beam per transceiver chain per time slot. The utilization of subband-specific analog beams offers a new opportunity in designing mmWave systems, allowing for enhanced cell capacity and reduced pilot overhead. To understand the practical feasibility of JPTA, a few challenges and system design considerations are discussed in relation to the performance and complexity of the JPTA systems. For example, frequency-selective beam gain losses are present for the subband analog beams, e.g., up to 1 dB losses for 2 subband cases, even with the state-of-the-art JPTA delay and phase optimization methods. Despite these side effects, system-level analysis reveals that the JPTA system is capable of improving cell capacity: the 5%-tile throughput by up to 65%.

**Index Terms**— mmWave, MIMO, beamforming, JPTA

## I. INTRODUCTION

Joint-phase time array (JPTA) radio frequency (RF) frontend architecture has been studied in various literatures [1-10], to offer frequency-selective analog beams in an orthogonal-frequency-division-multiplexing (OFDM) symbol, with a single digital transceiver chain (TRx). The analog beamforming constraint, i.e., one analog beam per TRx at a same time duration, is present in traditional mmWave base station (BS) design. With the constraint, the mmWave BS can only serve those users on a similar angular direction at each scheduling time slot, which has caused severe scheduling restrictions. The BS constructed with JPTA, on the other hand, can schedule multiple users per TRx towards different angular directions, in a frequency-division multiplexing (FDM) manner [1].

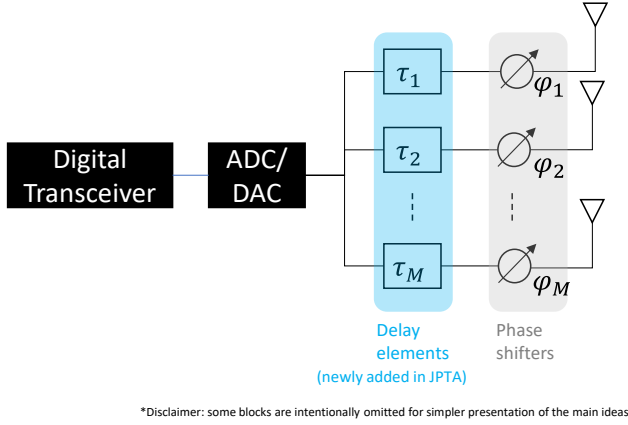
Exploiting the relaxation of the scheduling restriction, JPTA has a good potential help increasing data channel throughput and reducing overhead. However, to realize the JPTA benefits in practical BS systems, performance and complexity aspects need to be carefully studied.

As for complexity, specific algorithms relying on heavy computational operations, like iterative algorithms [1,12], will be more difficult to be conducted per time slot, while other algorithms utilizing a closed form solution [9] could be easier to be implemented online. However, the practical feasibility of generating these JPTA parameters per scheduling time slot depends on specific implementations of the BS, e.g., digital processing architecture and real-time computational capacity, control bandwidth and latency to set beam weight values to beamforming integrated chips (BF-IC), etc. Hence, this paper does not intend to make a statement on whether specific algorithms are feasible for real-time implementation or not.

On the other hand, performance can be analyzed with simpler assumptions on the implementation options, and hence this paper focuses on characterizing performance benefits of JPTA. The performance of different JPTA parameter determination algorithms will be analyzed with a *beam-gain-loss* metric, which can be easily translated into received signal to noise ratio (SNR) and block error rate (BLER). To understand the ultimate system throughput benefits of JPTA, *system-level analysis* will be used with modeling a BS and its serving user terminals (UTs), wireless channel propagations, user scheduling and physical-layer abstractions.

The outline of this paper is as in the following. In Section II, JPTA RF front-end architecture and a problem formulation to determine delay and phase parameters to construct frequency-selective analog beams will be covered. In Section III, the use cases and benefits of JPTA architecture will be introduced. In Section IV, BS system design considerations will be presented to realize the JPTA benefits. In Section V, a system-level JPTA performance study will be presented, with demonstrating throughput gain of JPTA against traditional single-TRx systems. There, various algorithms to derive JPTA parameters to construct desired beam patterns will be considered, and their

> REPLACE THIS LINE WITH YOUR MANUSCRIPT ID NUMBER (DOUBLE-CLICK HERE TO EDIT) <



(a) JPTA RF frontend architecture

**Frequency-selective phase tuning**

$$\mathbf{x}_k = \begin{bmatrix} e^{j(2\pi f_k \tau_1 + \phi_1)} \\ e^{j(2\pi f_k \tau_2 + \phi_2)} \\ \vdots \\ e^{j(2\pi f_k \tau_M + \phi_M)} \end{bmatrix} \mathbf{s}_k \triangleq \mathbf{p}_k s_k$$

Delay element values      Phase shifter values

$k$	subcarrier index
$f_k$	subcarrier frequency
$M$	total number of antennas
$m$	antenna index
$\tau_m$	delay value associated with antenna $m$
$\phi_m$	phase value associated with antenna $m$
$\mathbf{x}_k$	an $M \times 1$ equivalent signal vector at subcarrier $k$
$\mathbf{p}_k$	an $M \times 1$ equivalent precoding vector at subcarrier $k$
$s_k$	a modulation symbol at subcarrier $k$

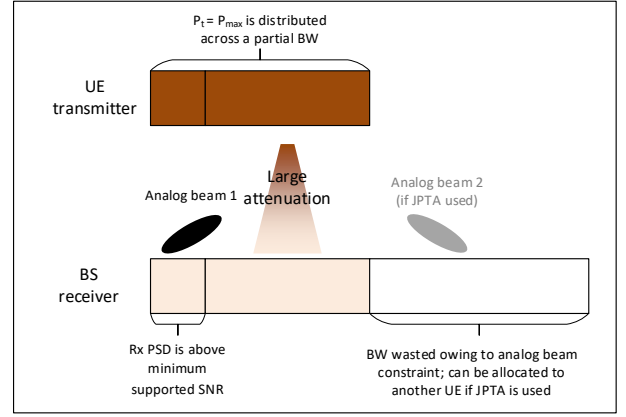
(b) Equivalent frequency-domain signal model

Figure 1. JPTA frontend architecture and an equivalent signal model in the frequency domain

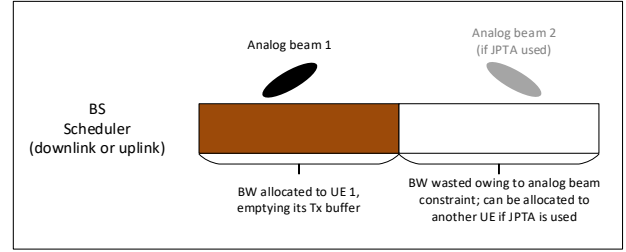
beam-gain loss performance will be presented. In Section VI, a concluding remark and future study areas will be presented.

## II. FUNDAMENTALS OF JOINT PHASE TIME ARRAY

Joint phase time array (JPTA) radio frequency (RF) frontend architecture refers to the one shown in Figure 1. The main difference between the JPTA and conventional architecture is that controllable delay elements are appended to the RF phase shifters, which offer extra degrees of freedom to design analog beams. As time-domain delay translates into frequency-domain phase ramping, the delay values assigned to the delay components can be used to create frequency selectivity for the analog beams. According to the equivalent frequency-domain



(a) For FDM of power-limited UEs' transmissions



(b) For partially-loaded UEs

Figure 2. JPTA use cases for data channels

signal model presented in Figure 1, per-subcarrier beam patterns can be designed by tuning the delay and phase parameter values across the antennas. Typically, the JPTA parameter determination problem is formulated with digital Fourier transform (DFT) weights steering to specific directions for individual frequency sub-bands as desired frequency-domain beam weights. For example, to steer a beam to  $\theta$  in elevation angle, the DFT weights along the antennas placed on a vertical axis of a 2-dimensional uniform rectangular array will be determined according to  $\exp(-j2\pi m \cos \theta)$ , where  $m \in \{0, \dots, M-1\}$  is an antenna index. Utilizing these DFT weights, an optimization problem is formulated to minimize the sum of the magnitude squared errors between the DFT beam weights and  $\mathbf{x}_k$  across all  $k$ .

## III. USE CASES AND SYSTEM BENEFITS

By exploiting frequency-selective analog beams constructed with JPTA, a base station can be designed to simultaneously serve multiple users in different angular locations in a frequency-division multiplexing (FDM) manner, with a single digital transceiver chain. On the other hand, JPTA has limitations over conventional multiple transceiver systems, as JPTA does not offer spatial multiplexing on the same frequency band. Still, JPTA has its unique advantage over the multiple transceiver systems, as it does not require power-hungry

> REPLACE THIS LINE WITH YOUR MANUSCRIPT ID NUMBER (DOUBLE-CLICK HERE TO EDIT) <

multiple analog-to-digital & digital-to-analog converters (ADC/DAC) and other related components. Hence, JPTA is a cost-effective alternative for scheduling multiple users in different angular directions in the same time duration.

In this sequel, we will discuss system design possibilities with JPTA and the potential benefits of these designs.

#### A. Data Channels

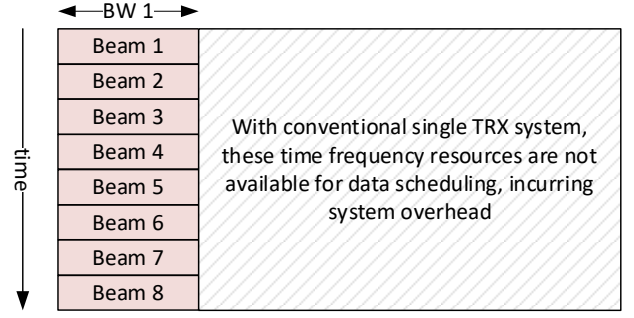
As JPTA does not support multi-user multi-input-multi-output (MIMO) antenna spatial multiplexing transmissions, the peak spectral efficiency of a JPTA system remains the same as a conventional single-TRx system. However, JPTA helps to achieve extra cell capacity in certain cases, namely for power-limited uplink transmissions and for partially loaded UTs as illustrated in Fig. 2.

The use case for power-limited UTs studied is shown in Fig. 2(a). To comply with industry standards and meet regulatory requirements, UT's maximum transmission power shall not exceed a certain value, say  $P_{\max}$ . Suppose that a power-limited UT is configured to transmit with  $P_{\max}$ . In such a case, the serving BS typically also limits the UT's transmission BW to ensure successful demodulation of a transmitted data channel with a minimum required signal-to-noise ratio (SNR) despite the expected channel attenuation. When the UT's scheduled transmission BW is smaller than the system bandwidth and conventional analog beam constraint is imposed, the left-over bandwidth is wasted if no users are available in the same angular direction as the power-limited UT. With JPTA, the BS can allocate the remaining bandwidth to other UTs in different angular directions, which leads to improved cell throughput. Also, as power-limited UTs are scheduled more frequently with JPTA, a UT's UL throughput at a given location increases, or a target UL data rate can be achieved at a farther distance. Exploiting this, a new scheduler can be devised to maximize scheduling opportunities for individual users while allowing a reduction of per-user scheduling bandwidth. With the new scheduler, the overall user throughput increases further thanks to more scheduling opportunities and higher per-tone transmission power [2].

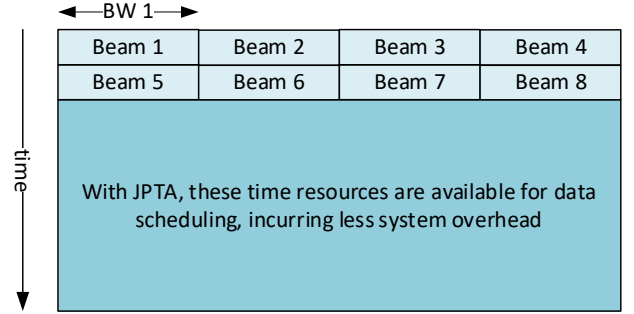
Fig. 2 (b) presents the use case for partially loaded UTs. With partial loading, the amount of data to be transmitted to or received by a UT is finite, sometimes insufficient to fill up the entire system BW. With JPTA, the left-over bandwidth can be scheduled for another UT in different angular locations, which helps to improve cell throughput and user perceived throughput.

#### B. Pilots and Overhead Channels

Frequency-selective analog beams generated with JPTA can be used for reducing overhead by multiplexing beams in the same time duration for beam management pilots and control channels [5], [7], [8], [10], [11], [13]. In conventional single TRx systems, these overhead channels are transmitted in such a way that a single beam is transmitted per time duration. When these overhead channels do not require full bandwidth usage for the scheduled time duration, the remaining bandwidth is wasted, as illustrated in Fig. 3(a). With JPTA, on the other hand,



(a) In conventional single-TRx systems



(b) In systems with JPTA

Figure 3. Multiplexing beams in conventional single TRx systems vs. JPTA systems

these overhead channels intended for users on different angular locations are scheduled with these frequency selective analog beams in the same time duration, as presented in Fig. 3(b). Accordingly, more full-bandwidth time resources are open for data transmissions, which can be used to increase cell throughput. In the context of 3<sup>rd</sup> generation partnership project (3GPP) standards [14], pilot channels correspond to synchronization signal blocks (SSBs), channel-state-information reference signals (CSI-RS), etc.; and control channels correspond to physical uplink control channels (PUCCH), physical downlink control channels (PDCCH).

#### IV. SYSTEM DESIGN CONSIDERATIONS WITH JPTA

In this section, overall BS system design aspects are presented, to realize the performance and overhead benefits envisioned in Section III.

To perform FDM of data channels with different beams as explained in Section III-A, the BS needs to know the best beams for different UTs and other conventional scheduling parameters for the UTs, e.g., buffer status, channel condition, etc. Such information is readily available in single TRx conventional systems, relying on beam management and channel state information (CSI) feedback constrained on single TRx operations as defined in 3GPP [14]. If the JPTA delay values can be dynamically set to zero as well as non-zero values, the FDM of data channels can be achieved with non-zero delay values while relying on conventional beam management and

> REPLACE THIS LINE WITH YOUR MANUSCRIPT ID NUMBER (DOUBLE-CLICK HERE TO EDIT) <

CSI feedback procedures with zero delay values. This can be an attractive option that can be used for the JPTA BS's acquiring the necessary beam and scheduling information, to reduce initial implementation complexity.

To schedule a JPTA data channel for a time slot, multiple pairs of a scheduling subband (SB) and a beam angle need to be determined to serve multiple UTs. Having individual UTs' scheduling parameters, the BS can rely on traditional scheduling metrics, e.g., proportional fair metrics, to choose a primary user to schedule. The rest of the bandwidth can be allocated to other UTs even if they are on different beam directions, considering tradeoffs among cell capacity, fairness, priority, etc. To further improve user throughput, the BS scheduler may want to reduce the primary user's scheduling bandwidth with the intention of increasing per-user scheduling opportunities [2].

The feasibility of the online generation of JPTA parameters for arbitrary BW-beam pairs depends upon various implementation constraints. In a system where online JPTA parameter configuration is not feasible, a lookup table of JPTA parameters can be utilized. The lookup table can be constructed offline to contain JPTA beams and their parameters for allowable BW-beam pairs.

For reducing hardware design costs, spatial-domain simplification can also be considered. Instead of having one delay component per antenna to make the JPTA beams distributed in both azimuth and elevation directions, the JPTA system can be constructed with one delay component for each column of the uniform rectangular antenna array to make JPTA beams distributed across the azimuth domain only. Again, this incurs extra scheduling constraints, but the adverse impact is marginal. Because power-limited users are at the cell edge in limited elevation beam ranges, the JPTA beams across the azimuth domain on cell-edge elevation beams can be used to improve cell capacity and coverage for cell-edge users.

## V. NUMERICAL PERFORMANCE ANALYSIS

This section presents a numerical performance analysis that reveals the practical performance benefits of JPTA compared to baseline phased antenna array systems.

For this purpose, an intuitive performance metric for the "goodness of fit" is introduced and evaluated to compare various alternative algorithms to derive the JPTA parameters, namely *average beam gain loss*. The frequency-selective analog beams constructed with JPTA typically exhibit reduced beam gains within the desired subbands. The decoding performance of frequency-selective fading channels can be characterized by the average SNR across the frequency subband [2]. The average SNR in dB is linearly dependent upon the average beam gain loss in dB. *Hence, the smaller the beam gain loss, the better the block error rate.*

The analysis is on a JPTA use case of uplink throughput enhancement, particularly for cell-edge users.

### A. System Model

A single-TRx BS is equipped with a 24V16H antenna array, with each antenna element (AE) controlled by a 6-bit tunable phase shifter. The system operates at a bandwidth of 400 MHz with a sub-carrier (SC) spacing of 120 kHz. The BS's horizontal scan range extends 120°, and the vertical scan range covers 25°, divided uniformly across 126 beams (18 rows and 7 columns).

Two JPTA architectures are analyzed: three-dimensional (3D) JPTA and azimuth-only (AO) JPTA. In 3D JPTA [12], each AE is paired with an adjustable delay element, enabling frequency-dependent beamforming across both azimuth and elevation planes. In contrast, AO JPTA connects each column of antennas to a single delay element—yielding a total of 16 delay elements—allowing frequency-dependent beamforming only in the azimuth plane, with elevation control handled by phase shifters. While 3D JPTA offers increased beamforming flexibility, it requires more delay elements to achieve its functionality.

### B. Beam-Gain Loss

JPTA beam design algorithms vary in terms of performance and complexity. Options include a closed-form least squares (LS) solution in [9] (extended to 3D in [12]) for low complexity, an iterative algorithm [1] offering a balanced performance-complexity trade-off, and a gradient descent (GD) approach [12] providing high beam gains at the cost of increased computational complexity. The choice of beam design algorithm depends on the BS's computational resources and whether online or offline beam design is feasible. Effective beam gain for JPTA is computed by averaging dB beam gains across SCs assigned to each UT.

Table I presents beam gain losses (in dB) evaluated for different algorithms and beam configurations based on simulations of 100,000 UTs uniformly distributed in the angular domain. The GD algorithm, as expected, achieves the lowest beam gain loss—up to 1.5 dB less at the 90th percentile—though it demands higher computational power. The iterative algorithm achieves a 1 dB improvement over LS, balancing performance with lower complexity. In particular, the 90%-tile beam gain loss remains below the 3 dB and 6 dB bounds for two-beam and four-beam configurations, respectively. Here, 3 dB and 6 dB bounds represent the beam gain losses from constructing 2 and 4 beams with a single set of phase shifters without introducing JPTA. Additionally, Table I highlights the maximum delay required to achieve the desired beam patterns, observed below 10 ns, which sets a requirement for the delay component design to construct up to 4-beam JPTA systems for 400 MHz operational bandwidth [15].

Between 3D and AO configurations, 3D achieves lower beam gain loss. This can be attributed to the additional degrees of freedom in the 3D configuration, which employs extra delay elements to support beamforming across both azimuth and elevation. These added elements enable more precise beam shaping, thus minimizing gain loss compared to the AO approach.

> REPLACE THIS LINE WITH YOUR MANUSCRIPT ID NUMBER (DOUBLE-CLICK HERE TO EDIT) <

Table I: JPTA beam gain loss in dB

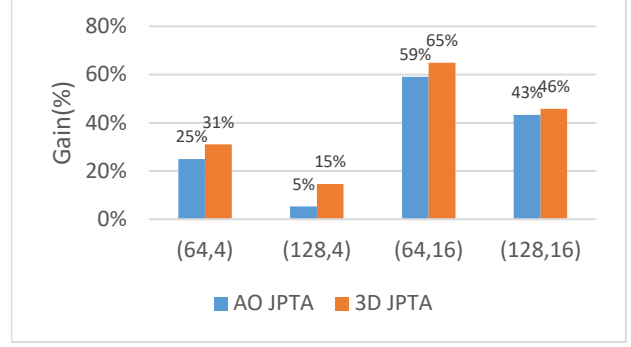
JPTA Type	# of beams	Algorithm	90%-tile (dB)	Mean (dB)	Max delay (ns)
AO	2	LS	1.04	0.84	3.5
		Iterative	1.03	0.80	3.5
		GD	1.00	0.79	3.5
	4	LS	4.65	2.67	9
		Iterative	3.41	2.03	9
		GD	3.22	2.00	9
3D	2	LS	0.99	0.98	3.5
		Iterative	1	0.95	4
		GD	0.99	0.94	4
	4	LS	4.56	3.34	9.5
		Iterative	3.5	2.56	9.5
		GD	3.2	2.53	9.5

### C. System Throughput Analysis

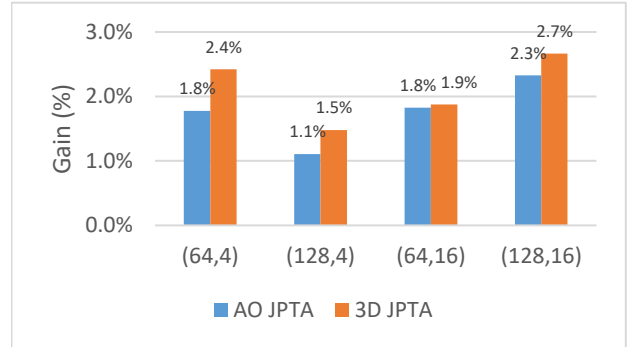
A system-level simulation is conducted to evaluate JPTA's impact on throughput. The study area is a 3 km radius around a site in Flower Mound, TX, USA, containing 5,000 houses within range, and wireless channels of BS-UT links were generated by ray-tracing simulations. Fixed wireless access (FWA) scenario is evaluated, where each house features wall-mounted customer premises equipment (CPE) with a single-TRx 8V8H array aligned toward the strongest BS path, achieving an effective isotropic radiated power (EIRP) of 51 dBm. For each evaluation, out of the 5000 CPEs, a pool of  $N_{pool}$  CPEs is randomly selected. For simplicity, round-robin scheduling of up to  $N_{max}$  CPEs is conducted per scheduling time slot to model BS scheduling and beamforming constraints.

For the baseline, CPEs are scheduled together only when the same beam serves them. For AO JPTA, CPEs are scheduled together if the same elevation beams serve them, while in 3D JPTA, CPEs are scheduled together without restrictions on their serving beams. In JPTA, priority in scheduling the secondary CPEs is given to those served by the same beam as the primary CPE, then to CPEs on the same row of beams on the same elevation, and then for 3D JPTA, the rest of the UTs. This priority hierarchy minimizes beam gain loss and activates JPTA selectively.

To intuitively understand the impact of JPTA on UT throughput, cell-edge UTs with low signal-to-noise ratios (SNRs) operating over a narrow bandwidth (tens of SCs) are considered. For these UTs, throughput is approximated using Shannon's formula as  $B T \text{SNR}$ , where  $B$  is the UT bandwidth,  $T$  is the time fraction allocated to the UT, and SNR assumes the full beamforming gain of  $10 \log_{10} N_t$ . Under JPTA, the



(a) 5%-tile Throughput



(b) Average Throughput

Figure 4. Throughput gain of AO and 3D JPTA for different  $(N_{pool}, N_{max})$  combinations

throughput expression becomes  $\frac{B T N_{beams} \text{SNR}}{l(N_{beams})}$ , where  $N_{beams}$  represents the UT multiplexing factor and  $l(N_{beams})$  accounts for beam gain reduction. This implies that JPTA enhances performance for cell-edge UTs as long as  $\frac{N_{beams}}{l(N_{beams})} > 1$ . For example, in two-beam (four-beam) scenarios, beam gain loss must remain below 3 dB (6 dB) for JPTA to be beneficial.

To understand the impact of JPTA on all UTs, figure 4 presents mean and 5%-tile throughput gains for different  $(N_{pool}, N_{max})$  combinations, relative to traditional phase-only beamforming, with JPTA beam count capped at four. For fixed  $N_{max}$ , increasing  $N_{pool}$  generally reduces JPTA throughput gains, as more CPEs may share the same beam, reducing the need for JPTA. In the AO-JPTA example, the 5%-tile throughput gain drops from 25% to 5% when the CPE density doubles with a fixed  $N_{max}=4$ . Conversely, increasing  $N_{max}$  for a fixed  $N_{pool}$  enhances JPTA throughput gains, as fewer CPEs are likely to be served by the same beam. In the AO-JPTA example, the 5%-tile throughput gain increases from 5% to 43% when  $N_{max}$  increases from 4 to 16 for a fixed UT density. Thus, JPTA performance improves when the BS can schedule more CPEs per slot, supporting the use of low-complexity scheduling and beamforming algorithms.

JPTA delivers improvements in average throughput and 5%-tile throughput (representing cell-edge CPEs), as shown in Figure 4.

> REPLACE THIS LINE WITH YOUR MANUSCRIPT ID NUMBER (DOUBLE-CLICK HERE TO EDIT) <

High-SNR users achieve limited benefit from JPTA, as they are not power-limited and can utilize increased transmission opportunities in the time domain as effectively as additional bandwidth. Conversely, cell-edge UTs, constrained by instantaneous power limitations, benefit from increased transmission time, even if it comes with reduced bandwidth. This enhancement for cell-edge UTs effectively expands broadband coverage, addressing the common constraint of uplink throughput in FWA scenarios. These trends hold consistently across both AO and 3D JPTA configurations, highlighting JPTA's impact on improving uplink performance, particularly for cell-edge users. Compared to AO JPTA, 3D JPTA achieves higher throughput gains due to its lower beam gain loss (as shown in Table I) and increased flexibility in UT scheduling. However, 3D JPTA's requirement for more delay elements introduces a performance-cost trade-off, balancing enhanced throughput with added hardware complexity.

## VI. CONCLUDING REMARKS

This paper introduced system benefits, system design considerations, and system performance of mmWave base station (BS) systems equipped with Joint Phase Time Array (JPTA) radio-frequency (RF) frontend architecture. With JPTA, BS is capable of scheduling multiple devices in different spatial directions in the same time slot, with alleviating traditional analog beamforming constraints. The frequency selective beams formed by the JPTA systems were proposed to be used to improve data channel coverage and capacity, and to reduce overhead and latency for beam management. Then practical system design constraints were discussed, and various options to reduce system design complexity was discussed, e.g., azimuth-only JPTA instead of three dimensional JPTA. System-level simulation results confirmed that JPTA improves average and cell-edge throughput, with the most substantial gains observed at the cell edge (up to 65% throughput gain), often constrained in fixed-wireless-access settings. The findings showed that high-SNR users see minimal impact, while cell-edge users benefit more from JPTA due to the increased transmission time.

To further improve the JPTA BS system, at least the following three main categories of future works can be considered: (1) real-time JPTA parameter computation methods to achieve better tradeoff between complexity and beam-gain-loss complexity; along with hardware innovation to allow for larger control bandwidth to make real-time beam weight transfer to beamforming integrated circuits feasible; (2) lookup table optimization for offline computed JPTA parameters – for a given JPTA beam book size, what JPTA beams should be stored? (3) new standards protocol designs to facilitate JPTA features across the BS and devices, e.g., pilot design, control signaling to facilitate JPTA data transmissions and receptions, etc.

## REFERENCES

[1] V. V. Ratnam, J. Mo, A. AlAmmouri, B. L. Ng, J. Zhang, and A. F. Molisch, "Joint phase-time arrays: A paradigm for frequency-dependent analog beamforming in 6G," *IEEE Access*, vol. 10, pp. 73 364–73 377, Jul. 2022.

[2] A. AlAmmouri, J. Mo, V. V. Ratnam, B. L. Ng, R. W. Heath, J. Lee, and J. Zhang, "Extending uplink coverage of mmWave and Terahertz systems through joint phase-time arrays," *IEEE Access*, vol. 10, pp. 88 872–88 884, Jul. 2022.

[3] L. Dai, J. Tan, Z. Chen, and H. V. Poor, "Delay-Phase Precoding for Wideband THz Massive MIMO," *IEEE Trans. on Wireless Commun.*, vol. 21, no. 9, pp. 7271–7286, Mar. 2022.

[4] B. Zhai, A. Tang, C. Peng, and X. Wang, "SS-OFDMA: Spatial-spread orthogonal frequency division multiple access for terahertz networks," *IEEE J. Sel. Areas Commun.*, vol. 39, no. 6, pp. 1678–1692, Jun. 2021.

[5] V. Boljanovic, H. Yan, C.-C. Lin, S. Mohapatra, D. Heo, S. Gupta, and D. Cabric, "Fast beam training with true-time-delay arrays in wideband millimeter-wave systems," *IEEE Trans. on Circuits and Systems I: Regular Papers*, vol. 68, no. 4, pp. 1727–1739, Feb. 2021.

[6] C.-C. Lin, C. Puglisi, E. Ghaderi, S. Mohapatra, D. Heo, S. Gupta, H. Yan, V. Boljanovic, and D. Cabric, "A 4-element 800 MHz-BW 29 mW true-time-delay spatial signal processor enabling fast beam-training with data communications," in *Proc. IEEE 47th Eur. Solid State Circuits Conf. (ESSCIRC)*, Grenoble, France, Sep. 2021, pp. 287–290.

[7] C.-C. Lin, C. Puglisi, V. Boljanovic, H. Yan, E. Ghaderi, J. Gaddis, Q. Xu, S. Poolakkal, D. Cabric, and S. Gupta, "Multi-mode spatial signal processor with rainbow-like fast beam training and wideband communications using true-time-delay arrays," *IEEE Journal of Solid-State Circuits*, vol. 57, no. 11, pp. 3348–3360, Jun. 2022.

[8] A. Wadaskar, V. Boljanovic, H. Yan, and D. Cabric, "3D rainbow beam design for fast beam training with true-time-delay arrays in wideband millimeter-wave systems," in *Proc. IEEE Asilomar Conference on Signals, Systems, and Computers*, CA, USA, Oct. 2021, pp. 85–92.

[9] I. K. Jain, R. Reddy Vennam, R. Subbaraman, and D. Bharadia, "mmflexible: Flexible directional frequency multiplexing for multi-user mmwave networks," in *IEEE INFOCOM*, New York City, NY, USA, May 2023, pp. 1-10.

[10] M. Cui, L. Dai, Z. Wang, S. Zhou and N. Ge, "Near-Field Rainbow: Wideband Beam Training for XL-MIMO," in *IEEE Trans. on Wireless Commun.*, vol. 22, no. 6, pp. 3899-3912, Jun. 2023

[11] R. Li, H. Yan, and D. Cabric, "Rainbow-link: Beam-alignment-free and grant-free mmW multiple access using true-time-delay array," *IEEE J. Sel. Areas Commun.*, vol. 40, no. 5, pp. 1692–1705, Jun. 2022.

[12] O. Yildiz, A. AlAmmouri, J. Mo, Y. Nam, E. Erkip, J. Zhang. "3D Beamforming Through Joint Phase-Time Arrays," in *IEEE 100th Vehicular Technology Conference (VTC2024-Fall)*, Oct. 2024. [Online]. Available: <https://arxiv.org/abs/2401.00819>

[13] C.-C. Lin, V. Boljanovic, H. Yan, E. Ghaderi, M. A. Mokri, J. J. Gaddis, A. Wadaskar, C. Puglisi, S. Mohapatra, Q. Xu, S. Poolakkal, D. Heo, S. Gupta, and D. Cabric, "Wideband beamforming with rainbow beam training using reconfigurable true-time-delay arrays for millimeter-wave wireless," *IEEE Circuits and Systems Magazine*, 22(4), pp.6-25, Oct. 2022

[14] 3GPP Technical Report 38.802, "Study on new radio access technology: physical layer aspects," version 14.2.0, September 2017

[15] J. Mo, A. AlAmmouri, S. Dong, Y. Nam, W. Choi, G. Xu, and J. Zhang, "Beamforming with Joint Phase and Time Array: System Design, Prototyping and Performance" in *Proc. IEEE Asilomar Conference on Signals, Systems, and Computers*, CA, USA, Oct. 2024



> REPLACE THIS LINE WITH YOUR MANUSCRIPT ID NUMBER (DOUBLE-CLICK HERE TO EDIT) <



**Young-Han Nam** (Member, IEEE) received Ph.D. from the Ohio State University in 2008, and MS and BS degrees from Seoul National University in 2002 and 1998. From 2008 to 2019, he was with Samsung Research America (SRA), making contributions to the 3GPP RAN1 standards on mmWave, massive MIMO, 5G channel modeling, etc. For 3GPP standardization, he served as a rapporteur for the 5G channel modeling study item, responsible for editing TR38.901. From 2019 to 2022, he was with Mavenir, overseeing O-RAN product R&D in the system engineering team. Currently, he serves as a Senior Director in SRA, leading 6G cellular communication system research.



**Ahmad AlAmmouri** (Member, IEEE) received the B.Sc. degree (Hons.) from the University of Jordan, Amman, Jordan, in 2014, the M.Sc. degree from the King Abdullah University of Science and Technology (KAUST), Thuwal, Saudi Arabia, in 2016, and the Ph.D. degree from The University of Texas at Austin, Austin, TX, USA, in 2020, all in electrical engineering. He is currently a Staff Research Engineer with Samsung Research America, Plano, TX, USA. He was awarded the Chateaubriand Fellowship from the French Embassy in the USA, in 2019, the Professional Development Award from UT Austin, in 2019, and the WNCG Student Leadership Award, in 2020. He was recognized as an Exemplary Reviewer from the IEEE TRANSACTIONS ON COMMUNICATIONS, in 2017, and from IEEE TRANSACTIONS ON WIRELESS COMMUNICATIONS, in 2017 and 2018.



**Jianhua Mo** (Senior Member, IEEE) received the B.S. and M.S. degrees from Shanghai Jiao Tong University in 2010 and 2013, respectively, and the Ph.D. degree from The University of Texas at Austin in 2017, all in electronic engineering. He is a Senior Staff Engineer with Samsung Research America, Plano, TX, USA. His research interests include physical layer security, MIMO communications with low-resolution ADCs, and mmWave beam codebook design and beam management. His awards and honors include the Heinrich Hertz Award in 2013, the Stephen O. Rice Prize in 2019, the Best Wi-Fi Innovation Award by Wireless Broadband Alliance (WBA) in 2019, an Exemplary Reviewer of the IEEE WIRELESS COMMUNICATIONS LETTERS in 2012, an Exemplary Reviewer of the IEEE COMMUNICATIONS LETTERS, in 2015, and the Finalist for Qualcomm Innovation Fellowship, in 2014.



**Jianzhong Charlie Zhang** (Fellow, IEEE) received the Ph.D. degree from the University of Wisconsin-Madison. He was with the Nokia Research Center, from 2001 to 2006, and Motorola, from 2006 to 2007. From 2009 to 2013, he was the Vice Chairman of 3GPP RAN1 WG. He is currently the Senior Vice President and the Head of the Standards and Mobility Innovation Laboratory, Samsung Research America, where he leads research, prototyping, and standards for 5G cellular systems and future multimedia networks.